RSC Advances

PAPER

View Article Online
View Journal | View Issue

Cite this: *RSC Adv.*, 2022, **12**, 15685

One-step coordination of metal–phenolic networks as antibacterial coatings with sustainable and controllable copper release for urinary catheter applications†

Zhimao Huang,‡[a] Dawei Zhang,‡[b] Qinwei Gu,[a] Jiru Miao,[a] Xiao Cen,[ac] Robert Petrovich Golodok,[d] Vadim Victorovich Savich,[d] Alexander Phyodorovich Ilyushchenko,[d] Zhansong Zhou*[b] and Rong Wang *[a]

Catheter-associated urinary tract infections (CAUTIs) draw great concern due to increased demand for urinary catheters in hospitalization. Encrustation caused by urinary pathogens, especially *Proteus mirabilis*, results in blocking of the catheter lumen and further infections. In this study, a facile and low-cost surface modification strategy of urinary catheters was developed using one-step coordination of tannic acid (TA) and copper ions. The copper content of the coating could be manipulated by the number of TA–Cu (TC) layers, and the coating released copper in a pH-responsive manner. The coating exhibited high antibacterial efficiency (killed >99% of planktonic bacteria, and reduced biofilm coverage to <1% after 24 h) due to the synergistic antimicrobial effect of TA and copper ions. *In vivo* study with a rabbit model indicated that with two TC layers, the coated catheter could effectively inhibit bacterial growth in urine and colonization on the surface, and reduce encrustation formation. In addition, the TC-coated catheter exhibited better tissue compatibility compared to the unmodified catheter, probably due to the antibacterial performance of the coating. Such a straightforward coating strategy with good *in vitro* and *in vivo* antibacterial properties and biocompatibility holds great promise for combating CAUTIs in clinical practice.

Received 15th March 2022
Accepted 17th May 2022

DOI: 10.1039/d2ra01675c

rsc.li/rsc-advances

1 Introduction

Implantable medical devices like urinary catheters have significantly improved healthcare quality, and therefore, the clinical demand for catheters is increasing.[1] However, the surface of an implanted urinary catheter provides an ideal site for bacterial invasion and proliferation, and consequently leads to substantially high incidence of catheter-associated urinary tract infections (CAUTIs) in the clinic. It has been reported that more than 62 700 urinary tract infections (UTIs) occurred in US hospitals in 2015,[2] and approximately 68% of UTIs in acute care hospitals are recognized as CAUTIs,[3] which lead to prolonged hospital stay, increased nosocomial cost, and high risk of mortality. Common pathogens, such as *Proteus mirabilis* (*P. mirabilis*), *Escherichia coli* (*E. coli*), and *Staphylococcus aureus* (*S. aureus*), invade and colonize on the catheter surface, form biofilms, and eventually establish infections in the urethral tract. *P. mirabilis*, which is an important uropathogen and produces the most abundant biofilms in chronic indwelling catheters,[4] could elevate urinary pH by releasing urease to hydrolyse the urea into ammonium, deposit calcium and magnesium ions as crystals, obstruct the urinary catheters and, consequently, result in pyelonephritis and even death.[5,6] Once crystals are precipitated and bacterial extracellular matrix is formed, the bacteria are protected from antimicrobial agents.[7,8] Therefore, prevention of bacterial infections and biofilm formation is essential for retarding encrustation on urinary catheters.

Surface modification of catheters with antifouling[9] or bactericidal moieties[10] exhibited good performance in

[a]*Zhejiang International Scientific and Technological Cooperative Base of Biomedical Materials and Technology, Zhejiang Engineering Research Center for Biomedical Materials, Cixi Institute of Biomedical Engineering, Ningbo Institute of Materials Technology and Engineering, Chinese Academy of Sciences, Ningbo 315300, China. E-mail: rong.wang@nimte.ac.cn*

[b]*Department of Urology, The Southwest Hospital, Army Medical University, No. 30 Gaotanyan Street, Shapingba District, Chongqing, 400038, China. E-mail: zzs68754186@tmmu.edu.cn*

[c]*State Key Laboratory of Oral Diseases & National Clinical Research Center for Oral Diseases, Department of Temporomandibular Joint, West China Hospital of Stomatology, Sichuan University, No. 14, 3rd Section, South Renmin Road, Chengdu, 610041, China*

[d]*SSI O V Roman Powder Metallurgy Institute, National Academy of Sciences of Belarus, Minsk, 220005, Belarus*

† Electronic supplementary information (ESI) available. See https://doi.org/10.1039/d2ra01675c

‡ These authors made equal contributions to this work.

suppressing bacterial adhesion and biofilm formation. However, planktonic bacterial cells in urine are also responsible for infection and increased risk of encrustation. The urinary tract environment is associated with extensive deposition of bacterial cells and/or crystals from the urine, which could block the surface and significantly impair the antibacterial efficacy of the coating. For this reason, coatings with release of antimicrobials including antibiotics,[11–13] silver,[14,15] and copper,[16–18] which could kill planktonic bacteria, are preferred in urinary catheter applications. However, the concerns on possible antibiotic resistance,[19] and high toxic effects of silver components[20] are becoming escalating issues recently. Compared with the silver compounds, the copper counterparts show lower toxicity and higher biosafety. The half maximal effective concentration (EC50) values of copper salts and nanoparticles for mammalian cells are 26.5 and 2.2 times that of silver salts and nanoparticles,[21] respectively. However, in conditions with high moisture or at body temperature, copper exhibited low antimicrobial efficacy,[22–24] limiting its application in biomedical devices. Therefore, strategy to develop copper-based antibacterial coatings with good cytocompatibility and promoted antimicrobial activity is needed.

Polyphenols, like tannic acid (TA), are plant-derived natural compounds with more than two phenolic groups, which can benefit human health for cancer prevention, anti-inflammatory, and antibacterial activity.[25] In addition, TA has been widely used in surface modification due to its various chemical and physical interactions with virtually arbitrary materials, including coordination with metals, hydrogen bonds and Michael addition and Schiff-base reactions.[26–28] TA has good biocompatibility, and is affirmed as Generally Recognized as Safe (GRAS) by the Food and Drug Administration (FDA). At high concentration, TA binds to peptidoglycan of the bacterial cell wall and interferes with integrity of bacterial membrane, causing lysis of the bacterial cells.[29] Metal ions like copper ions can be chelated with TA to obtain metal–TA coordinated coatings with enhanced antibacterial capability, and have shown potential in blood-contacting devices[30] and marine applications.[31] In addition to the antimicrobial activity, it has been reported that TA could reduce the activity of urease,[32,33] maintain an acidic condition of urine, and thereby inhibit the formation of encrustation. Taking advantage of the antimicrobial capability of TA and copper ions, and the simplicity of coordination chemistry of TA–Cu complexation, a facile strategy to construct an antibacterial TA–Cu (TC) coating on urinary catheter was developed in this study. Copper ions spontaneously chelated with TA to form a stable metal–polyphenol network on the surface. The copper content and release profile of copper ions were optimized by construction of a multi-layered TC coating *via* a repeated immersion process. The bacteria-killing and antibiofilm activity against Gram-positive *S. aureus*, and Gram-negative *E. coli* and *P. mirabilis*, and *in vitro* cytotoxicity of the TC coatings were investigated. *In vivo* antibacterial and anti-encrustation performance and tissue biocompatibility of the TC-coated urinary catheter were evaluated using a rabbit model.

2 Experimental section

2.1 Materials

Tannic acid (TA) was obtained from Aladdin Chemistry (Shanghai, China). Copper(II) sulfate, hydrochloric acid, nitric acid, and ammonium hydroxide were purchased from Sinopharm (Shanghai, China). Phosphate-buffered saline (PBS) was obtained from Phygene Life Sciences (Fujian, China). SYLGARD™ 184 Silicone Elastomer Kit was obtained from Dow Chemical Company (Michigan, United States), and used to prepare flat polydimethylsiloxane (PDMS) sheet (0.1 cm thickness) following the manufacturer's instruction. Silicone Foley catheter (8 Fr) was purchased from Wellead (Guangzhou, China). *P. mirabilis* 0317 and *S. aureus* 5622 were gifts from Ningbo University. *E. coli* ATCC 25922 was obtained from American Type Culture Collection. NIH/3T3 fibroblast cells (Category No. SCSP-515) were obtained from National Collection of Authenticated Cell Cultures (Shanghai, China). Cell Counting Kit-8 (CCK-8), and Calcein/PI Cell Viability/Cytotoxicity Assay Kit were purchased from Beyotime (Shanghai, China). LIVE/DEAD® *Bac*Light™ Bacterial Viability Kits L13152 was obtained from Thermo Fisher Scientific (Massachusetts, United States).

2.2 Surface modification

Flat PDMS substrates were cut into 1 cm × 1 cm × 0.1 cm sizes, and placed in a 5 mL centrifuge tube containing 4 mL solution of TA and $CuSO_4$ at various molar ratio, while the total concentration of TA and $CuSO_4$ was fixed at 3.76 mmol L^{-1}. The solution with the PDMS substrate was shaking in a constant temperature oscillator (THZ-98A, Bluepard) (100 rpm, 37 °C) for 24 h, washed thoroughly using deionized water and dried in nitrogen flow. The obtained TA–Cu-coated substrate was denoted as TC-1. The TC-1 substrate was immersed in 4 mL of the same freshly prepared TA–$CuSO_4$ solution for another 24 h under the same condition, washed with deionized water and dried in nitrogen flow. The obtained substrate was denoted as TC-2. A TA-coated substrate was prepared in the same manner with use of 4 mL of TA solution at the same TA molar concentration, instead of the TA–$CuSO_4$ solution. TC-2-coated catheter was prepared by treating a silicone Foley catheter (8 Fr, Wellead) in 500 mL of TA–$CuSO_4$ solution in a plastic container (5.5 cm in diameter and 30 cm in height) for 24 h, and then washed with copious amounts of deionized water, immersed in another freshly prepared TA–$CuSO_4$ solution for another 24 h, and collected as described above.

2.3 Surface characterization

Surface properties of the coatings were characterized using water contact angle measurement, atomic force microscopy (AFM), X-ray photoelectron spectroscopy (XPS), Fourier transform infrared (FTIR) spectroscopy and UV-visible absorption spectroscopy with 1 cm × 1 cm × 0.1 cm flat PDMS samples rather than curved catheters. The complex of TA–Cu in the reacted solution was collected and analyzed using ^{1}H nuclear magnetic resonance (NMR) and liquid chromatography-

quadrupole-time-of-flight mass spectrometry (LC-Q-TOF-MS). The experimental details are given in the ESI.†

2.4 Copper content and *in vitro* release profile

Copper content of TC-1 and TC-2 samples and *in vitro* copper cumulative release of TC-2 samples at different pH over 7 days were determined by inductively coupled plasma-optical emission spectrometry (ICP-OES, SPECTRO ARCOS, AMETEK). TC-1 and TC-2 samples with size of 1 cm × 1 cm × 0.1 cm were digested in a glass bottle containing 3 mL of 13 mol L^{-1} HNO_3 and 1 mL deionized water for 3 h, and then the solution was diluted to 50 mL for Cu quantification. For the Cu release study, pH of the PBS buffer (initial pH 7.2) was adjusted to 4.0 using 13 mol L^{-1} HCl or 10.0 using 25–28 wt% $NH_3 \cdot H_2O$. TC-2 sample was immersed in 2 mL of PBS buffer with different pH values in a 5 mL centrifuge tube. After shaking at 37 °C and 100 rpm for 24 h, 1.5 mL of the PBS solution was taken and replaced with 1.5 mL of fresh PBS buffer. The collected PBS solution was stored at 4 °C for ICP-OES measurement. Three replicates were measured for each sample.

2.5 Antibacterial assay

Bacteria were cultured in appropriate broth at 37 °C overnight, shaking at 100 rpm (*E. coli* and *P. mirabilis* in lysogeny broth and *S. aureus* in tryptic soy broth). To investigate the antibacterial property of the coating in a time-dependent manner, a 1 cm × 1 cm × 0.1 cm sample was incubated in 2 mL of PBS suspension containing approximate 10^6 cells per mL of bacteria at 37 °C, and shaking at 100 rpm. At the time points of 0, 3, 6, 12, and 24 h, the viable bacterial cells in the suspension were counted using the spread plate method. Three replicates were measured for each sample. For the biofilm formation assay, the bacterial culture was diluted 5000 times with the fresh broth and 1 mL of the suspension was added in each well of a 24-well-plate containing 1 cm × 1 cm × 0.1 cm PDMS sample. The plate was sealed with parafilm and incubated at 37 °C for 3 days. The broths were replaced with fresh ones every 24 h. After incubation, the bacterial culture was discarded and washed by 1 mL deionized water for 3 times in each well to remove any loosely adhered cells. The samples were transferred to another new plate. For scanning electron microscopy (SEM) observation, the bacterial cells on PDMS surface were fixed by adding 1 mL 2.5% glutaraldehyde solution, incubated at room temperature for 2 h, and followed by stepwise dehydration using 1 mL of 25%, 50%, 75%, 90% and 100% ethanol for each step. The samples were dried and coated with Au under ion sputtering (MC1000, Hitachi). The bacterial cells on the substrate surface were observed using SEM (Regulus 8230, Hitachi). The biofilm coverage on surface was determined by ImageJ software (version 1.53a). Three replicates were measured for each sample. For confocal laser scanning microscopy (CLSM, TCS SP8, Leica) observation, bacterial cells on the surface were stained using a combined dye (LIVE/DEAD® *Bac*Light™ Bacterial Viability Kits, L13152, Thermo Fisher Scientific) following the manufacturer's instruction. The sample was kept in dark for 15 min, washed with 1 mL deionized water and transferred to a BeyoGold™ 35 mm confocal dish. The sample was observed under CLSM (TCS SP8, Leica) with a 488 nm laser source and SYTO Green and propidium iodide dye channels.

2.6 Cytotoxicity assay

The cytotoxicity assay was tested according to ISO 10993-5. To extract any potentially toxic component, a flat PDMS sheet (pristine or coated, 1 cm × 1 cm × 0.1 cm in size) was placed in a 15 mL tube with 2 mL Dulbecco's Modified Eagle Medium (DMEM, supplemented with 10% fetal bovine serum, 10^5 U L^{-1} penicillin and 100 mg L^{-1} streptomycin) at 37 °C for 24 h. Meanwhile, NIH/3T3 fibroblasts were seeded in a 96-well-plate at a concentration of 10^4 cells per well. After incubation at 37 °C for 24 h, the cell culture medium was replaced with 100 μL of the sample extracts, and the cells were incubated for another 24 h. In the control groups, the culture medium was replaced with 100 μL of fresh DMEM. Viability of the cells in each well was determined using CCK-8 assay according to the manufacturer's protocol. To investigate cell viability after co-culture with substrate, a 1 cm × 1 cm × 0.1 cm flat sample was placed in a 24-well-plate, which was filled with 1 mL of cell suspension (10^5 cells per mL). The cells were cultured at 37 °C for 24 h, followed by staining with the Calcein/PI Cell Viability/Cytotoxicity Assay Kit according to the manufacturer's instruction, and then observed using CLSM.

2.7 *In vivo* implantation study

All studies in rabbits were approved by the Ethics Committee of the First Affiliated Hospital of Army Medical University, and all surgical procedures and post-operative care were supervised by the staff of the Animal Center of First Affiliated Hospital of Army Medical University. Male New Zealand rabbits (2.0–2.5 kg) were used for *in vivo* studies. Before implantation, pristine and TC-2-coated catheters were sealed in packages and sterilized by ethylene oxide following the procedures stated in ISO 11135:2014. After anaesthesia, the belly hair of the rabbit was shaved. The area of 5 cm in diameter around the rabbit's genital was disinfected with iodophor. The catheter was inserted through the urethra into the bladder of the rabbit in a sterile condition. Five mL sterile saline was injected to enlarge the balloon of the catheter. After the catheterization, the external part of the catheter was fixed to the belly of the rabbit by sewing. An Elizabethan collar was attached to the animal's neck to prevent it from biting the catheter during the wake. Catheters were observed every day to check whether they were blocked. Seven days after catheterization, urine and blood from the animal was collected, and the animal was sacrificed to collect the catheter and relevant organs (*i.e.* urethra, bladders). The blood was subjected for complete blood count test. The bacteria in the urine and on the catheter surface were counted using spread plate method. The interested regions of the organs were excised, fixed in 10% formalin, and stained using hematoxylin and eosin (H&E, Solarbio G1120, China) for histological observation. The biofilms and crystals on the harvested catheters were subjected to SEM observation, and element qualification and quantification using Energy-Dispersive X-ray Spectroscopy (EDS) and ICP-OES as described above.

3 Results and discussion

3.1 Surface characterization

Polyphenols like TA provide multiple binding groups for chelation with metal ions to form a stable film on a range of substrate surfaces.[34] Typically, the phenolic group of TA can be deprotonated, and consequently act as a ligand for metal cations such as iron(III)[34] and copper(II).[30] Herein, TA–Cu (TC) coating was constructed on the surfaces of the flat PDMS substrate as well as the silicone catheter through coordination of TA and copper ion in a simple immersion process (Scheme 1a and b). Formation of TA–Cu complex was confirmed by the FTIR spectra (Fig. S1†), in which the peak of C_{Ar}–OH at 3000–3700 cm^{-1} in TC coating decreased, compared to that of TA coating, due to the consumption of C_{Ar}–OH in the metal coordination process. ^1H NMR spectrum showed the proton signal of phenolic hydroxyls of the TA–Cu complex decreased (Fig. S2†), and LC-Q-TOF-MS results confirmed the formation of stable TA–Cu complex (Fig. S3†). Coating with solutions containing TA and Cu ions at a TA/Cu molar ratio of 1 : 3 was found to have the highest absorbance at 291 nm, which is a typical peak of TA–Cu complex (Fig. S4†). Further increase of the TA/Cu molar ratio did not increase the absorbance of the TC coating on PDMS surface. Therefore, an optimal TA/Cu molar ratio of 1 : 3 in the TA–Cu solution was used in the rest of the study for preparation of TC coating. Multi-layered TC coating can be constructed through a simple repeated immersion process (Scheme 1a). A slightly brown film was observed on the catheter surface after two TA–Cu coating steps (Scheme 1c).

Chemical compositions of the substrate surface after different coating steps were determined by XPS (Fig. 1a). While no copper signal was observed on PDMS and TA-coated surfaces, TC-1 and TC-2 surfaces showed small Cu 2p peaks at ~933 eV and ~953 eV, indicating the successful modification of the surface with TA–Cu coating. The pristine PDMS surface showed a C–H peak at 284.8 eV and a C–Si peak at 285.6 eV. After TA treatment, the C–Si peak at 285.6 eV significantly decreased

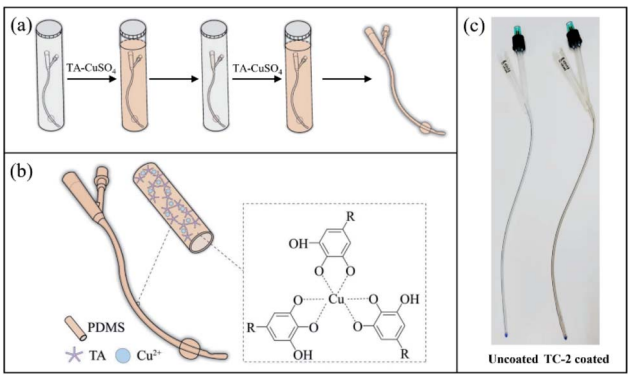

Scheme 1 Schematic illustration of (a) fabrication of tannic acid–copper (TC) coating on silicone catheter surface *via* a repeated immersion process, and (b) chemical structure of TC network on silicone catheter surface. (c) Photographs of unmodified and TC-2-coated catheters. The unmodified catheter was colourless, and the TC-2-coated catheter had slightly brown film on the surface.

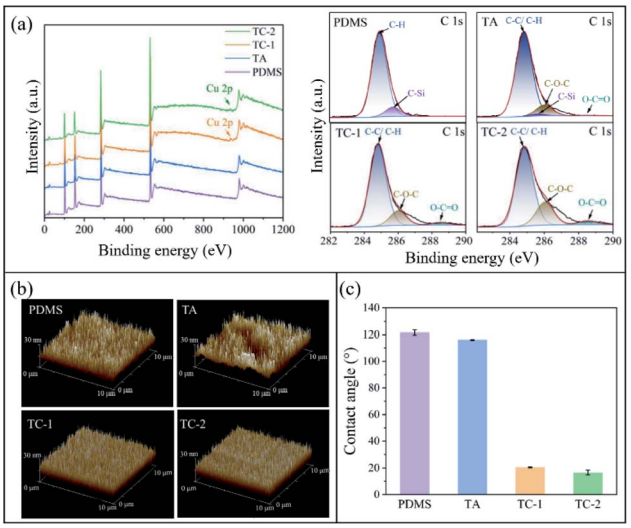

Fig. 1 Surface characterization of different surfaces: (a) XPS wide-scan spectra and C 1s core-level spectra, (b) AFM 3D images, and (c) water contact angles of pristine and TA- and TC-modified PDMS surfaces.

and peaks at 286.0 eV (C–O–C peak) and 288.5 eV (O–C=O peak) appeared. The ratio of C–O–C peak to C–C/C–H peak on TA coating was 0.128, and it increased to 0.180 and 0.297 on TC-1 and TC-2 surfaces, respectively, probably due to that the polyphenol–metal coordination promoted TA deposition in TC-1 and TC-2 coatings. With another step of TA–Cu coating, the C–O–C and O–C=O peaks further increased, indicating more TA molecules were deposited on the TC-2 surface. AFM observation showed that the TC-1 and TC-2 surfaces were smooth compared to the pristine PDMS and TA-coated surfaces (Fig. 1b), indicating that TA–Cu chelation could result in a homogeneous coating. TA coating reduced the surface contact angle slightly from 121.55 ± 1.95° of pristine PDMS to 116.01 ± 0.35° of TA-coated surface (Fig. 1c). This value was higher than those reported in the previous study,[35] probably due to a relatively low concentration of TA used in the surface modification in this study. In contrast, the water contact angle was significantly decreased to 20.04 ± 0.26° and 16.53 ± 1.80° on the TC-1 and TC-2 surfaces, respectively. The results from XPS, AFM and water contact angle measurements confirmed that the TA–Cu chelation resulted in a homogeneous coordination network and promoted TA deposition on the surface.

3.2 Copper content and *in vitro* release

The copper content of TC-1 and TC-2 coatings was determined using ICP-OES (Fig. 2a). The copper content of TC-2 coating (2.333 ± 0.063 μg cm^{-2}) was nearly 3.5 times that of the TC-1 coating (0.675 ± 0.075 μg cm^{-2}), indicating a higher coverage of TA–Cu coating on TC-2 surface. *In vitro* release of copper ions from TC-2 surface was investigated by incubation of the substrate in PBS with different pH values and the released copper concentration was measured using ICP-OES (Fig. 2b). The copper release in neutral pH was 0.187 μg cm^{-2} in the first day, and the ultimate copper release reached 0.499 μg cm^{-2} over

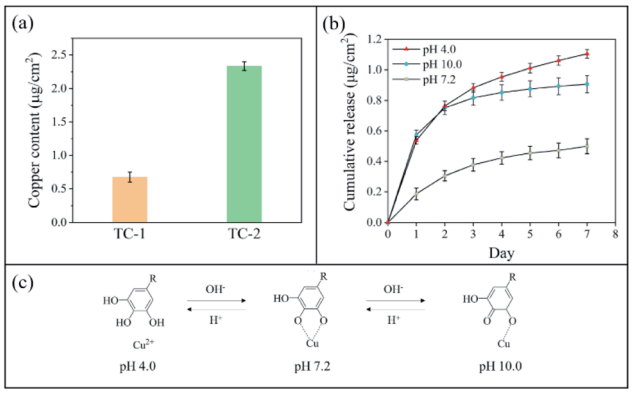

Fig. 2 (a) Copper content of TC-1 and TC-2-coated silicone substrates, and (b) copper release from 1 cm × 1 cm TC-2-coated silicone substrate after incubation in 2 mL PBS buffer at different pH over 7 days at 37 °C and quantified by ICP-OES. (c) pH-responsive transition of TA–Cu network.

7 days. However, in PBS with pH 4.0 and 10.0, the copper release was significantly increased to 0.537 μg cm^{-2} and 0.574 μg cm^{-2} in the first day, respectively, and the release rate decreased in the following six days. The cumulative copper release at pH 4.0 and 10.0 was 1.105 μg cm^{-2} and 0.907 μg cm^{-2} in seven days, which approximately doubled that at neutral pH (0.499 μg cm^{-2}). The pH-responsive behaviour of copper release from TC-2 coating was probably due to the protonation and deprotonation of hydroxyl groups in TA upon change of pH (Fig. 2c). At acidic pH, the hydroxyl groups in TA were protonated, leading to disassembly of the TA–Cu network. Consequently, copper ions were dissociated from the metal–catechol coordination complex. At alkaline pH, parts of the phenol groups were oxidized to quinone, which has lower affinity to Cu ions, resulted in disassembly of the TA–Cu network.[34,36,37] This could confer the coating with enhanced antibacterial capability in scenario with elevated pH, and is likely to be beneficial for application in inhibiting *P. mirabilis*-associated infections and encrustation.[5,6]

3.3 Antibacterial activity

The surface of indwelling catheter provides an initiation site of bacterial infection as bacterial cells could invade the urethra and bladder through catheter lumen. Without appropriate control treatments, the bacterial cells on catheter surface could proliferate and secrete extracellular polymeric substances (EPS) to form biofilm.[19] The TC-2 coating effectively killed common uropathogens including *P. mirabilis*, *E. coli* and *S. aureus* in a time-dependent manner (Fig. S5†). After 3 h of incubation with TC-2 coating, >97% of *P. mirabilis*, and >99% of *E. coli* and *S. aureus* in the suspension were killed. Furthermore, the killing efficiency of the TC-2 coating against all the three bacterial species increased to >99% after 24 h. Biofilm formation on pristine and modified PDMS substrates was further investigated. As can be seen, the surface of pristine PDMS was heavily colonized by the challenging bacteria after 24 h (Fig. 3a), and the biofilm coverage reached 60.08% for *P. mirabilis*, 71.89% for *E. coli* and 67.86% for *S. aureus* (Fig. 3b). The bacterial biofilm further developed and formed a higher coverage on the surface after 3 days of culture (Fig. S6†). The biofilm coverage of PDMS increased to 69.01% for *P. mirabilis*, 73.68% for *E. coli* and 79.96% for *S. aureus* after 3 days of culture (Fig. 3b). The TA coating partly inhibited biofilm formation, and the biofilm coverage at 24 h decreased to 39.64% for *P. mirabilis*, 47.44% for *E. coli* and 50.16% for *S. aureus*. The surface morphology and hydrophilicity did not change much after TA coating on PDMS surface in this study (Fig. 1b and c), so the antibacterial property

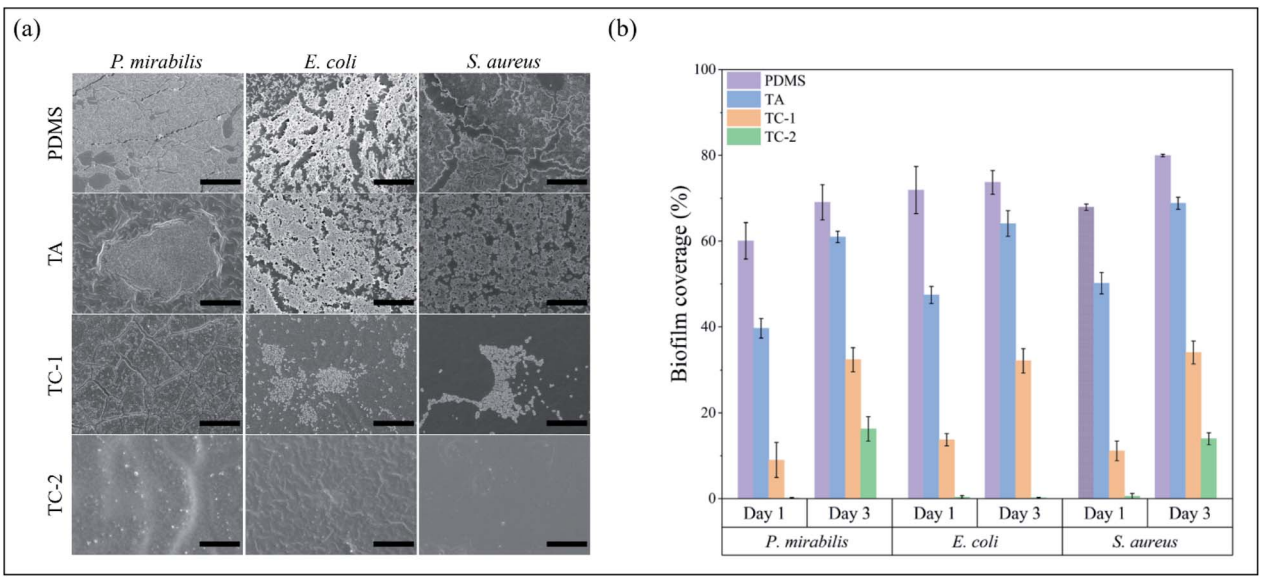

Fig. 3 *In vitro* antibacterial properties of different surfaces: (a) SEM images of bacterial biofilm of *P. mirabilis*, *E. coli* and *S. aureus* on the pristine and modified PDMS surfaces after incubation for 24 h. Scale bars represent 30 μm. (b) Biofilm coverage on pristine and modified PDMS surfaces after incubation in bacterial culture medium for 24 h and 72 h.

could probably be attributed to bioactivity of TA on the surface. However, the biofilm continuously to mature, and it inevitably covered the TA coating after 72 h (Fig. S6†). The biofilm coverage of TA increased by a large margin to 61.01% for *P. mirabilis*, 64.11% for *E. coli* and 68.81% for *S. aureus* (Fig. 3b). The TC-1 coating effectively inhibited bacterial biofilm formation over 24 h, and the biofilm coverage was reduced to 9.01% for *P. mirabilis*, 13.71% for *E. coli* and 11.13% for *S. aureus*. However, further culture of the bacteria still showed growth of the biofilm on the TC-1 surface (Fig. S6†), indicating low inhibitory efficacy of the coating, probably due to the low content of the antibacterial agents in the coating. All of the three species of microorganisms could hardly form biofilm on TC-2 coating (biofilm coverage below 1% after 24 h of culture). The TC-2 surface maintained relatively clean even after 72 h of culture and showed great inhibition against *E. coli* (biofilm coverage 0.19%). The biofilm coverage of TC-2 against *P. mirabilis* and *S. aureus* increased to 16.28% and 13.97%, respectively (Fig. 3b). The minimum inhibitory concentrations (MICs) of TA and $CuSO_4$ against *P. mirabilis* were determined to be higher than 512 μg mL^{-1}, while the value of TA–$CuSO_4$ combination against *P. mirabilis* reduced to 512 μg mL^{-1}, indicating there is a synergistic effect of TA and copper ions against the bacteria. CLSM images of *E. coli*, *P. mirabilis* and *S. aureus* biofilm exhibited the consistent tendency with SEM images on the various surfaces (Fig. S7†). After 3 days of incubation, the pristine PDMS failed to prevent biofilm formation. In contrast, TC-2 coating inhibited the formation of biofilms, which had reduced signal levels of bacteria compared with unmodified PDMS. In sum, the TC coatings exhibited strong inhibitory capability against common uropathogens, probably due to the dual antibacterial functions of TA and Cu^{2+} ions.

3.4 *In vitro* cytotoxicity

Fibroblast cells were seeded on the surface of pristine and TC-2 substrate. Very few cells were found adhering on the PDMS surface (Fig. 4a). This is because the cells have low affinity to the hydrophobic surface of PDMS.[38] In contrast, cells on TC-2 surface were mostly alive and mature in spindle-shape, indicating that TC-2 surface has rather low cytotoxicity and good compatibility and affinity to mammalian cells. The quantification results from the cytotoxicity assay showed that the extract medium obtained from the pristine and various coated substrates with a surface area/medium volume (SA/Vol) ratio of 1.2 cm^2 mL^{-1} has minimal cytotoxicity to fibroblasts (Fig. 4b). It should be noted that the copper released from 1 cm^2 of TC-2 coating in 2 mL PBS buffer (pH 7.2) over 24 h was estimated to be 0.249 μg mL^{-1}, which is relatively lower than the reported EC50 value of copper salts to mammalian cells (53 μg mL^{-1} on metal basis).[21] The coating with such low copper release rate but good antibacterial activity and biocompatibility showed great potential for indwelling biomedical device applications like urinary catheters.

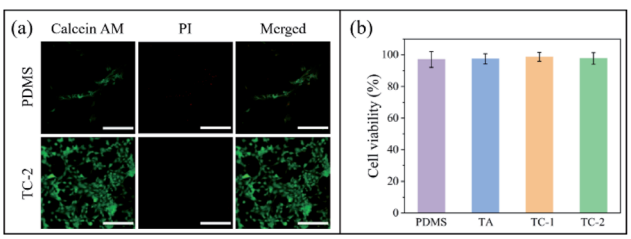

Fig. 4 (a) CLSM images of NIH/3T3 fibroblast cells co-cultured on pristine and modified PDMS sheets for 24 h. Scale bars represent 300 μm. (b) Cell viability of NIH/3T3 fibroblast after incubated in sample extracts for 24 h.

3.5 *In vivo* implantation study

Since the TC-2 coating exhibited excellent *in vitro* antibacterial performance and rather low cytotoxicity, TC-2-coated silicone catheter was implanted into a rabbit model for 7 days to further evaluate the *in vivo* performance (Fig. 5a). After 7 days of catheterization, the urine and catheter were collected (Fig. 5b). It could be observed that the outer surface of unmodified catheter in the distal portion, which contact to the animal's urethra and bladder, was covered by the bloody detached tissues, indicating bleeding and necrosis probably caused by infections. In contrast, the surface of TC-2-coated catheter was relatively clean. The cross-section of the unmodified catheter was blocked, while the TC-2 catheter remained open. The bacterial number in urine and on catheter surface on Day 7 was quantified using the spread plate method (Fig. 5c). According to the definition by the Infectious Diseases Society of America (IDSA), bacteriuria could be diagnosed if the bacteria count in the urine is higher than 10^5 CFU mL^{-1}.[39] In this study, five rabbits were enrolled in each group. Two urine samples from the control group (with unmodified catheter) were heavily infected, while the number of bacteria in the urine of the rest three samples was in the range of 10^4 to 10^5 CFU mL^{-1}. For the TC-2-coated catheter group, three urine samples were heavily infected, but no bacteria were detected in the urine of the rest two samples. The bacterial number on the TC-2-coated catheter surface was generally lower than that on the unmodified catheter (Fig. 5c). It should be noted that due to the constraints of the study, the urine collection bag was not attached to the catheter, and the catheter remained open throughout the experiment. Bacteria from the external environment could invade and migrate *via* the catheter lumen, resulting in a naturally occurring infection in the animal. Overall, the TC-2 coating inhibited bacterial invasion and migration on the catheter surface, resulting in good antibacterial performance. In addition, relative higher number and percentage of monocytes in the animal's blood of the unmodified catheter group on Day 7 were observed (Fig. S8†), indicating the animal in the control group had a high risk of monocytosis,[40] probably due to the acute bacterial infections in the animal. The catheter lumen was observed using SEM and the elements deposited on the surface were analyzed (Fig. 6a). It can be observed that crystals were formed in the unmodified catheter, which contain a high amount of calcium and magnesium, indicating the formation of encrustation.[6] In contrast, the lumen of the TC-2-coated catheter was relatively clean and few crystals were found. The amounts of calcium and

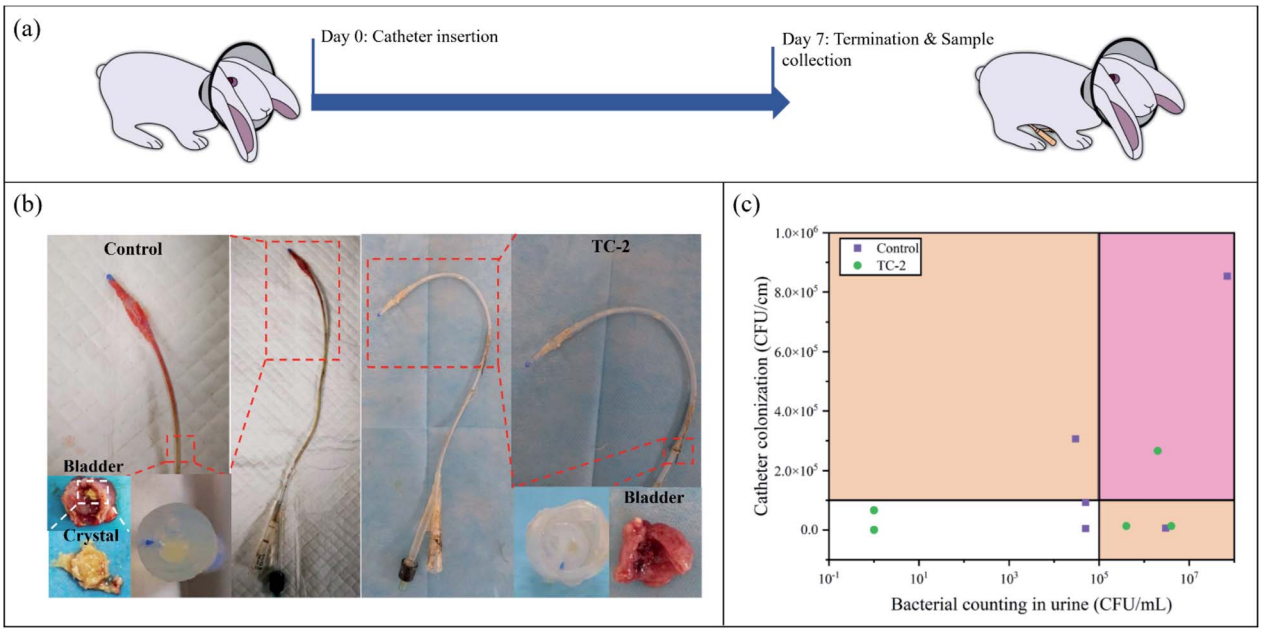

Fig. 5 (a) Schematic illustration of the animal study during 7 days of catheter implantation. (b) Photographs of catheter, bladder (with stones found in the bladder) and catheter lumen. (c) Bacteria counting on the surface of 1.5 cm-long catheter segments (5 cm away from the catheter tip) and in the urine of the unmodified catheter group and TC-2-coated catheter group on Day 7 ($n = 5$).

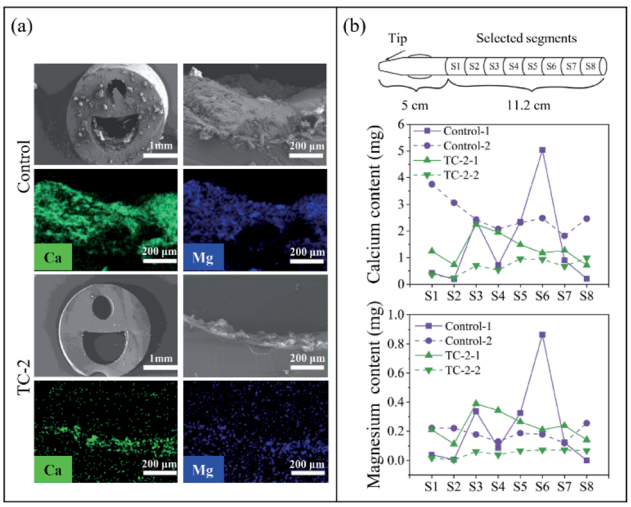

Fig. 6 (a) SEM images and EDS mapping of the lumen of unmodified and TC-2-coated catheters after implanted in rabbits for 7 days. The 1 mm-long catheter segments (5 cm away from the catheter tips) were collected. (b) Calcium and magnesium quantification on segments of the unmodified catheter and TC-2-coated catheter after implantation for 7 days. Eight 1.4 cm-long catheter segments (5 cm away from the catheter tip) of each catheter were collected for ICP-OES measurement ($n = 2$).

magnesium on the catheter surface were also determined using ICP-OES (Fig. 6b). As can be seen, the unmodified catheter group showed relatively higher content of calcium and magnesium than the TC-2-coated catheter, indicating the TC-2 coating inhibited the encrustation efficiently. Histological analysis of the bladder and urethra tissues indicated severer inflammation occurred and thickened and irregular transitional epithelium formed in the lower urinary tract of the group with unmodified catheter (Fig. 7a and b), compared with the group with TC-2-coated catheter (Fig. 7c and d). The bladder neck tissue of animal with unmodified catheter exhibited vacuolation in large area (Fig. 7a). Ammonia generated by hydrolysis of urea in urine could damage the protective glycosaminoglycan layer covered on urothelial cells, and induced severe bacteria invasion and encrustation.[7] The unmodified catheter failed to inhibit bacterial infections and encrustation, which could induce severe degree of inflammation. In contrast, the TC-2-coated catheter attenuated bacterial invasion and crystal formation, and thus resulted in a lower degree of inflammation in the surrounding tissues. Collectively, the TC-2 coating exhibited good *in vivo* antibacterial and anti-encrustation properties as well as excellent biocompatibility.

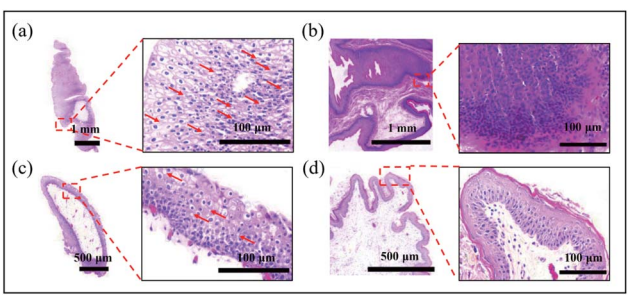

Fig. 7 Representative images of H&E stained (a) bladder neck and (b) urethra of the rabbit with unmodified catheter, and H&E stained (c) bladder neck and (d) urethra of the rabbit with TC-2-coated catheter after 7 days of implantation. The transitional epithelium was represented in the enlarged images. Vacuolation was marked by red arrows.

4 Conclusions

In this study, we developed a facile strategy to modify urinary catheter with an antibacterial, anti-encrustation, and biocompatible coating through metal–polyphenol coordinating chemistry. The copper content in the coating can be tuned by the multiple coating process, and the copper release from the coating was responsive to the environmental pH. The TC-2 coating exhibited excellent antibacterial activity against Gram-negative *P. mirabilis* and *E. coli*, and Gram-positive *S. aureus*, probably due to the synergistic antimicrobial activity of TA and Cu ions. No significant cytotoxicity of the coating to mammalian cells was observed. The animal study showed that the TC-2-coated urinary catheter has good biocompatibility, and effectively inhibited bacterial infection and encrustation over 7 days of implantation. Therefore, the TC-2 coating has great potential for modification of urinary catheters in combating CAUTIs in clinic practice.

Author contributions

Z. Huang developed the basic concept, conducted the experiments of surface modification and characterization, analyzed the data and wrote the manuscript. D. Zhang performed the animal experiments and analysis of data. Q. Gu performed the *in vitro* cytotoxicity assay. J. Miao and X. Cen assisted in performing the experiments and analysis of data. R. P. Golodok, V. V. Savich and A. P. Ilyushchenko reviewed and edited the manuscript. Z. Zhou supervised, reviewed and edited the manuscript. R. Wang contributed to development of the basic concept, supervision, review and editing the manuscript.

Conflicts of interest

There are no conflicts to declare.

Acknowledgements

This work was funded by the National Key Research and Development Program of China (2018YFE0119400), National Natural Science Foundation of China (51803229, 52011530019), Youth Innovation Promotion Association CAS (2021296), and S&T Innovation 2025 Major Special Program of Ningbo (2018B10040).

References

1 L. Liu, H. Shi, H. Yu, S. Yan and S. Luan, *Biomater. Sci.*, 2020, **8**, 4095–4108.
2 S. S. Magill, E. O'Leary, S. J. Janelle, D. L. Thompson, G. Dumyati, J. Nadle, L. E. Wilson, M. A. Kainer, R. Lynfield, S. Greissman, S. M. Ray, Z. Beldavs, C. Gross, W. Bamberg, M. Sievers, C. Concannon, N. Buhr, L. Warnke, M. Maloney, V. Ocampo, J. Brooks, T. Oyewumi, S. Sharmin, K. Richards, J. Rainbow, M. Samper, E. B. Hancock, D. Leaptrot, E. Scalise, F. Badrun, R. Phelps and J. R. Edwards, Emerging Infections Program Hospital Prevalence Survey Team, *N. Engl. J. Med.*, 2018, **379**, 1732–1744.
3 Virginia Department of Health Homepage, **https://www.vdh.virginia.gov/surveillance-and-investigation/hai/organisms/uti-and-cauti/**, retrieved May 2022.
4 L. E. Nicolle, *Antimicrob. Resist. Infect. Control*, 2014, **3**, 23.
5 D. J. Stickler and R. C. Feneley, *Spinal Cord*, 2010, **48**, 784–790.
6 D. J. Stickler, *J. Intern. Med.*, 2014, **276**, 120–129.
7 H. Hedelin, *Int. J. Antimicrob. Agents*, 2002, **19**, 484–487.
8 S. Saint and C. E. Chenoweth, *Infect. Dis. Clin.*, 2003, **17**, 411–432.
9 S. P. Nikam, P. Chen, K. Nettleton, Y. H. Hsu and M. L. Becker, *Biomacromolecules*, 2020, **21**, 2714–2725.
10 H. Yu, L. Liu, X. Li, R. Zhou, S. Yan, C. Li, S. Luan, J. Yin and H. Shi, *Chem. Eng. J.*, 2019, **360**, 1030–1041.
11 W. Zhou, Z. Jia, P. Xiong, J. Yan, Y. Li, M. Li, Y. Cheng and Y. Zheng, *ACS Appl. Mater. Interfaces*, 2017, **9**, 25830–25846.
12 S. Bakhshandeh, Z. Gorgin Karaji, K. Lietaert, A. C. Fluit, C. H. E. Boel, H. C. Vogely, T. Vermonden, W. E. Hennink, H. Weinans, A. A. Zadpoor and S. Amin Yavari, *ACS Appl. Mater. Interfaces*, 2017, **9**, 25691–25699.
13 S. K. Alsaiari, M. A. Hammami, J. G. Croissant, H. W. Omar, P. Neelakanda, T. Yapici, K. V. Peinemann and N. M. Khashab, *Adv. Healthcare Mater.*, 2017, **6**, 1601135.
14 H. Yang, G. Li, J. W. Stansbury, X. Zhu, X. Wang and J. Nie, *ACS Appl. Mater. Interfaces*, 2016, **8**, 28047–28054.
15 X. He, K. Gopinath, G. Sathishkumar, L. Guo, K. Zhang, Z. Lu, C. Li, E. T. Kang and L. Xu, *ACS Appl. Mater. Interfaces*, 2021, **13**, 20708–20717.
16 Z. Zhu, Q. Gao, Z. Long, Q. Huo, Y. Ge, N. Vianney, N. A. Daliko, Y. Meng, J. Qu, H. Chen and B. Wang, *Bioact. Mater.*, 2021, **6**, 2546–2556.
17 Y. Xu, S. Zhao, Z. Weng, W. Zhang, X. Wan, T. Cui, J. Ye, L. Liao and X. Wang, *ACS Appl. Mater. Interfaces*, 2020, **12**, 54497–54506.
18 J. Xiao, Y. Zhou, M. Ye, Y. An, K. Wang, Q. Wu, L. Song, J. Zhang, H. He, Q. Zhang and J. Wu, *Adv. Healthcare Mater.*, 2021, **10**, e2001591.
19 P. Tenke, B. Kovacs, M. Jackel and E. Nagy, *World J. Urol.*, 2006, **24**, 13–20.
20 E. Rezvani, A. Rafferty, C. McGuinness and J. Kennedy, *Acta Biomater.*, 2019, **94**, 145–159.
21 O. Bondarenko, K. Juganson, A. Ivask, K. Kasemets, M. Mortimer and A. Kahru, *Arch. Toxicol.*, 2013, **87**, 1181–1200.
22 D. Mitra, E. T. Kang and K. G. Neoh, *ACS Appl. Mater. Interfaces*, 2020, **12**, 21159–21182.
23 S. Jaiswal, P. McHale and B. Duffy, *Colloids Surf., B*, 2012, **94**, 170–176.
24 R. Mohan, A. M. Shanmugharaj and R. Sung Hun, *J. Biomed. Mater. Res., Part B*, 2011, **96**, 119–126.
25 C. Hano and D. Tungmunnithum, *Medicines*, 2020, **7**, 26.
26 B. J. Ortiz, J. Jennings, W. S. Gross, T. M. A. Santos, T.-Y. Lin, D. B. Weibel and D. M. Lynn, *Chem. Mater.*, 2021, **33**, 5401–5412.

27 Y. Zhao, R. Liu, Y. Fan, B. Zhao, W. Qian, J. Guo, C. Li, S. Chen, G. Luo, H. Deng and J. Zhang, *Chem. Eng. J.*, 2021, **425**, 130621.
28 J. Ren, R. Kong, Y. Gao, L. Zhang and J. Zhu, *J. Colloid Interface Sci.*, 2021, **602**, 406–414.
29 B. Kaczmarek, *Materials*, 2020, **13**, 3224.
30 X. Li, P. Gao, J. Tan, K. Xiong, M. F. Maitz, C. Pan, H. Wu, Y. Chen, Z. Yang and N. Huang, *ACS Appl. Mater. Interfaces*, 2018, **10**, 40844–40853.
31 J. Li, J. Li, J. Wei, X. Zhu, S. Qiu and H. Zhao, *ACS Appl. Mater. Interfaces*, 2021, **13**, 10446–10456.
32 C. E. Deutch, *J. Appl. Microbiol.*, 2017, **122**, 1380–1388.
33 S. M. Jones, T. T. Dang and R. Martinuzzi, *Int. J. Antimicrob. Agents*, 2009, **34**, 360–364.
34 H. Ejima, J. J. Richardson, K. Liang, J. P. Best, M. P. van Koeverden, G. K. Such, J. Cui and F. Caruso, *Science*, 2013, **341**, 154–157.
35 X. Lv, L. Wang, J. Fu, Y. Li and L. Yu, *New J. Chem.*, 2020, **44**, 15140–15147.
36 Y. Qin, J. Wang, C. Qiu, Y. Hu, X. Xu and Z. Jin, *ACS Sustainable Chem. Eng.*, 2019, **7**, 17379–17389.
37 X. Wang, J. Wu, P. Li, L. Wang, J. Zhou, G. Zhang, X. Li, B. Hu and X. Xing, *ACS Appl. Mater. Interfaces*, 2018, **10**, 34905–34915.
38 Y. J. Chuah, Y. T. Koh, K. Lim, N. V. Menon, Y. Wu and Y. Kang, *Sci. Rep.*, 2015, **5**, 18162.
39 L. E. Nicolle, K. Gupta, S. F. Bradley, R. Colgan, G. P. DeMuri, D. Drekonja, L. O. Eckert, S. E. Geerlings, B. Koves, T. M. Hooton, M. Juthani-Mehta, S. L. Knight, S. Saint, A. J. Schaeffer, B. Trautner, B. Wullt and R. Siemieniuk, *Clin. Infect. Dis.*, 2019, **68**, e83–e110.
40 A. A. Mangaonkar, A. J. Tande and D. I. Bekele, *Curr. Hematol. Malig. Rep.*, 2021, **16**, 267–275.